https://doi.org/10.1016/j.sse.2017.07.009

Effect of Post-Annealing on Sputtered MoS_2 films

W.C. Wong, S.M. Ng, H.F. Wong, W.F. Cheng, C.L. Mak and C.W. Leung*

Department of Applied Physics, The Hong Kong Polytechnic University, Hung Hom, Kowloon, Hong Kong, People's Republic of China

* email: dennis.leung@polyu.edu.hk

Abstract

Typical routes for fabricating MoS_2-based electronic devices rely on the transfer of as-prepared flakes to target substrates, which is incompatible with conventional device fabrication methods. In this work we investigated the preparation of MoS_2 films by magnetron sputtering. By subjecting room-temperature sputtered MoS_2 films to post-annealing at mild conditions (450°C in a nitrogen flow), crystalline MoS_2 films were formed. To demonstrate the compatibility of the technique with typical device fabrication processes, MoS_2 was prepared on epitaxial magnetic oxide films of $La_{0.7}Sr_{0.3}MnO_3$, and the magnetic behavior of the films were unaffected by the post-annealing process. This work demonstrates the possibility of fabricating electronic and spintronic devices based on continuous MoS_2 films prepared by sputter deposition.

Keywords: post-annealing; MoS_2; transfer-free

Highlights:

- MoS_2 films were deposited by magnetron sputtering and followed by post-annealed.
- Room-temperature sputtered MoS_2 films with post-annealing yielded strong Raman signals
- Transfer-free MoS_2 preparation was demonstrated, compatible with device fabrication processes

Introduction

The successful preparation of graphene and fabrication of related devices started the intensive research of two-dimensional (2D) materials including transition metal dichalcogenides (TMDs) [1, 2], silicene [3, 4] and phosphorene [5, 6]. Similar to graphene, TMDs are layer-structured materials that show high stability in air as compared with silicene and phosphorene. Depending on the structure and composition, they demonstrate semiconducting (MoS_2, WS_2), superconducting ($NbSe_2$) or semi-metallic (VS_2) behaviour.

MoS_2 is one of the first 2D-TMDs prepared, through the method of mechanical exfoliation [1]. Various electronic devices such as transistors, phototransistors [7] and gas detectors [8] based on mechanically exfoliated MoS_2 were investigated. The method of mechanical exfoliation relies on repeated thinning of bulk 2D materials by Scotch tape [9], and is useful for investigating new layered materials for research purposes. For example, monolayer crystals can be transferred to different substrates or other TMDs to produce van der Waals heterostructures [10]. However, the monolayer flakes so prepared are typically very small (< 10 μm) and with uncontrolled number of layers, and require the use of electron beam lithography for preparing electrodes and produce simple devices. The low yield rate of useable 2D flakes prepared by mechanical exfoliation is another drawback of the technique. Alternatively, TMDs can be chemically exfoliated, which has higher yield of monolayer TMD as compared with mechanical exfoliation; on the other hand, chemically exfoliated flakes are even smaller, which is suitable for preparing composites [11, 12] but is highly undesirable for making electronic devices.

Chemical vapor deposition (CVD) is the method of choice for producing large-area MoS_2. CVD of MoS_2 involves chemical reactions between Mo precursors (Mo metal or MoO_3) and S source (S, H_2S) under high temperature (> 700°C) [13-15]. The MoS_2 produced can then be wet-transferred onto different substrates.[16, 17] However, the wet-transfer process involves solvents that may contaminate the MoS_2/electrode interfaces. For example, the fabrication of vertical MoS_2 magnetic tunnel junctions by wet transfer method may trap contaminates between the MoS_2 and the magnetic layers. [17] The high temperature growth condition also limits the type of substrates onto which MoS_2 devices can be prepared.

Here, we report the preparation of MoS_2 using physical vapour deposition, namely the magnetron sputtering process. Sputter deposition of MoS_2 allows the preparation of highly continuous films with uniform coverage of target substrates over extended area, and is readily adaptable for industrial processes. For improving the crystallinity of the MoS_2 layers, an *ex situ* post-annealing process at moderate temperature (450°C) was adopted. Raman spectra of the samples exhibited good quality of the films. To demonstrate the applicability of the technique, we prepared MoS_2 on epitaxial perovskite manganite film of $La_{0.7}Sr_{0.3}MnO_3$, and the magnetic properties of the film was unaffected by the MoS_2 fabrication processes. The results suggest the applicability of the method in preparing high-quality MoS_2 layers, and is compatible with functional oxide materials for advanced electronic device applications.

Experimental

MoS_2 thin film layers were deposited on Si substrates by RF magnetron sputtering, with a target power of 50 W. The sputtering chamber was pumped down to 5 μTorr before deposition to suppress the oxidation of MoS_2. Sputtering took place under an Ar environment of 6 mTorr at room temperature. After the deposition, a post annealing process at 450°C was conducted *ex situ* with flowing nitrogen at atmospheric pressure for 30 minutes, in order to improve the crystallinity of the MoS_2 layer. The MoS_2 films were evaluated by Raman spectroscopy (Horiba HR800), using a laser with wavelength of 488 nm.

Results and Discussions

It was reported that laser annealing during Raman spectroscopy measurement can crystalize MoS_2 thin films sputtered at room temperature [18]. However, the finite laser spot size means that only localized crystallinity can be achieved; post-annealing the samples *ex situ* in a furnace should overcome such a size limitation issue. Fig. 1 shows the Raman spectra of 20 nm MoS_2 thin films after laser annealing and furnace annealing. Laser treatment of the MoS_2 film was conducted by illuminating the sample locally with the laser of Raman spectrophotometer system for 5 minutes (Red Curve). The laser power used was 180 mW and the spot size was ~1 μm. This is compared with the sample post-annealed *ex situ* at 450°C in a nitrogen flow (Black Curve). The Raman spectra show three peak, $E_{2g}^{\ 1}$ (383 cm^{-1}) and A_{1g} (408 cm^{-1}) peaks for MoS_2 and the Si substrate peak. The $E_{2g}^{\ 1}$ mode is a shear vibration mode within the MoS_2 plane, while the A_{1g} mode is the vertical vibration mode.[19] The full-width-at-half-maximum (FWHM) of the A_{1g} peak of furnace-annealed and laser-treated samples are 9 cm^{-1} and 12 cm^{-1}, respectively. The lower FWHM of furnace-annealed MoS_2 sample indicates its better crystallinity. The laser annealing process may not provide enough energy to increase the temperature for forming crystalline MoS_2.

We also note that the separation between $E_{2g}^{\ 1}$ and A_{1g} peaks is wide for furnace-annealed sample (25 cm^{-1}), as compared with the laser treated one (24 cm^{-1}). The laser-annealing process only affects MoS_2 film surface, and few-layered crystalline MoS_2 is formed. This result shows that the furnace annealing process can yield crystalline bulk MoS_2 films. Therefore furnace annealing was adopted for the following studies.

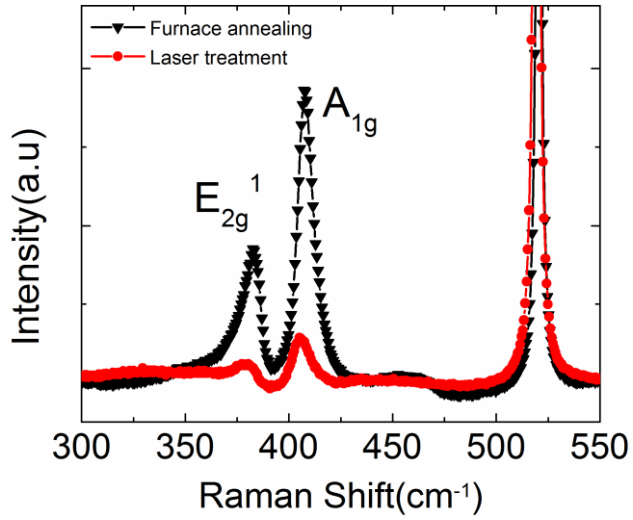

Fig.1 Raman spectra of furnace-annealed (black curve) and laser-annealed (red curve) MoS_2 films.

The sputtering temperature is an important parameter for determining the quality of resultant MoS_2 film. [20] Fig. 2a compares the 10-nm MoS_2 film deposited at room temperature (RT) before (black curve) and after (red curve) the furnace-annealing process. $E_{2g}^{\ 1}$ peak cannot be observed before the annealing process. Note that the $E_{2g}^{\ 1}$ mode is the shear vibration mode in a layer, and this result implies that layered structure cannot be established in RT-deposited MoS_2 film. The FWHM of A_{1g} peak before and after annealing are 11 cm^{-1} and 9 cm^{-1} respectively. The decrease of the FWHM indicates the annealing process leads to improved crystallinity of MoS_2 film. Moreover, $E_{2g}^{\ 1}$ mode was obtained after annealing, which means the layered structure was established by the annealing process.

In contrast, Raman measurements of MoS_2 film deposited at 500°C (Fig. 2b) shows no noticeable difference before (black curve) and after annealing (red curve). Note that the $E_{2g}^{\ 1}$ vibration mode can be obtained *before* annealing, which indicates the MoS_2 layers are already crystallized during the deposition process. The high temperature deposition can assist the crystallization process for MoS_2 film, hence the post-annealing treatment did not further improve the crystallinity.

Fig. 2c compares the Raman spectra of 10 nm MoS_2 films, which were deposited at RT (black curve) and 500°C (red curve) and followed by the post-annealing process. The FWHM of A_{1g} mode for post-annealed samples deposited at RT and 500°C are 9 and 16 cm^{-1}, respectively; such a difference in FWHM can be attributed to the vaporization of sulphur during the high temperature sputtering process, which leads to high sulphur vacancy in the sample. [21, 22] RT deposition can suppress the loss of sulphur during deposition and can be retained during atmospheric pressure post-annealing. In summary, RT-sputtered MoS_2 followed by post-annealing yields MoS_2 film with better crystallinity.

Fig. 2d show the effect of post-anealing temperature on the quality of RT sputtered MoS_2 films. While annealing at 300°C leads to marginal improvement on the Raman spectrum (as compared with the result in Fig. 2a), annealing at 450 °C clearly leads to an improved Raman signal from the MoS_2 sample. Post annealing at temperatures higher than 450°C has no apparent effect on the Raman spectrum.

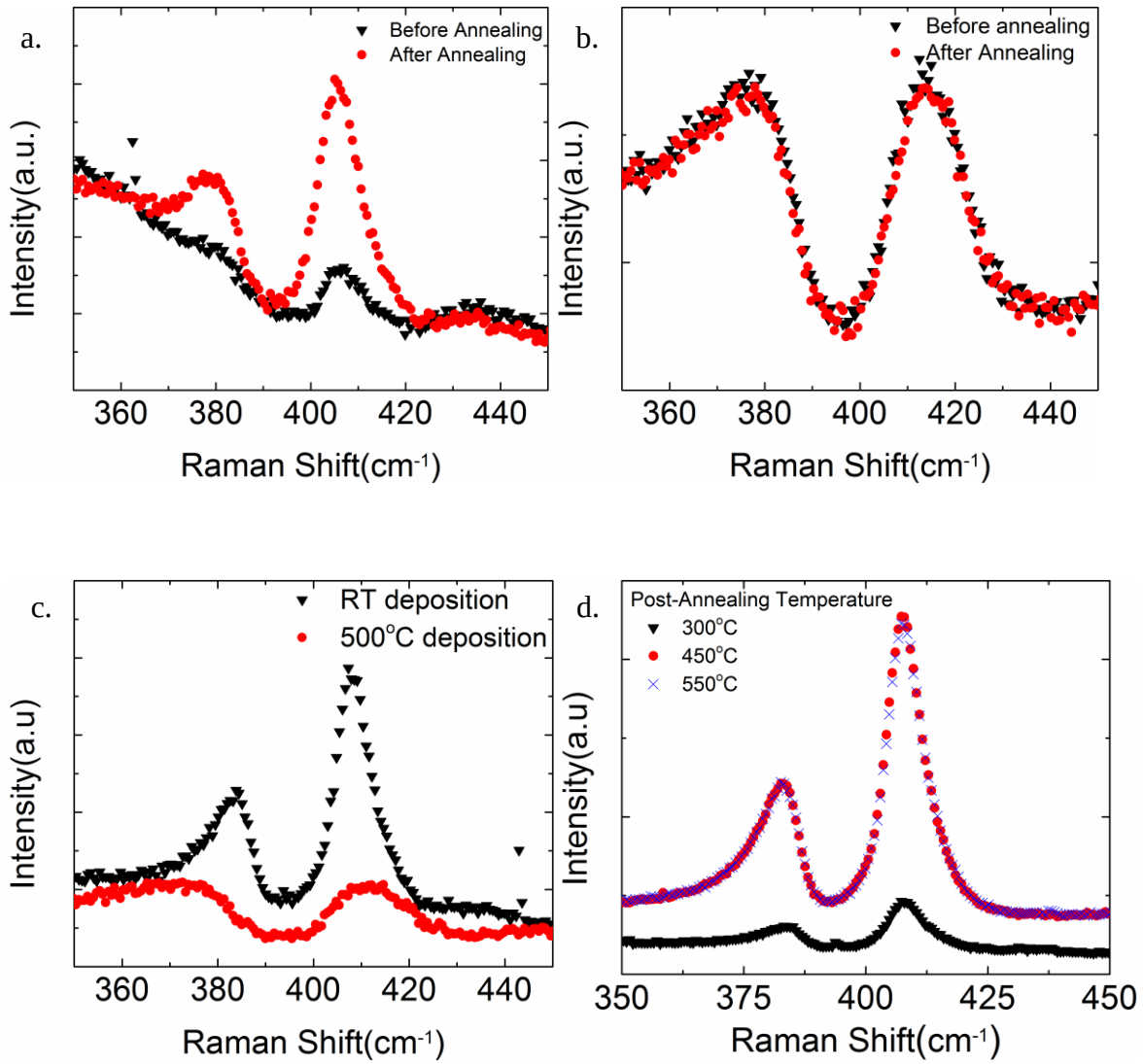

Fig. 2 Raman spectra of 10 nm MoS_2 films prepared and annealed under different conditions. (a) RT sputtered MoS_2 films before (black curve) and after (red curve) post annealing; (b) 500°C sputtered MoS_2 films before (black curve) and after (red curve) post annealing; (c) RT (black curve) and 500°C (red curve) deposited MoS_2 films after post-annealing. (d) RT deposited MoS_2 films post-annealed at different temperatures.

To demonstrate the applicability of the MoS_2 preparation technique for practical device fabrication processes, 2 nm MoS_2 was deposited on epitaxial $La_{0.7}Sr_{0.3}MnO_3$ (LSMO) (20 nm) films that were

grown by pulsed laser deposition on $SrTiO_3$ (STO) (001) single crystal substrates. LSMO is a magnetic oxide with magnetism that is highly sensitive to the oxygen vacancies in the films. The conditions for fabricating LSMO films were described previously.[23] Fig. 3 shows the Raman spectra of 2 nm MoS_2 film deposited on STO (red curve) and STO/LSMO (black curve). The board peak from 200 to 500 cm^{-1} is the STO substrate peak. The spectra show the MoS_2 E_{2g}^1 and A_{1g} modes superimposed on the substrate peak background. This means crystalline MoS_2 was successfully deposited on LSMO. The magnetic properties of LSMO were measured before and after the annealing process. The hysteresis loop of LSMO (Fig. 4) shows marginal difference before and after the post-annealing, an evidence for the unaltered magnetic properties during the annealing process. This result shows MoS_2 can be grown on LSMO without affecting its properties. Given the significance of LSMO in spintronic device research, the successful preparation of MoS_2 on LSMO allows the fabrication of novel electronic and spintronic devices bases on the associated materials.

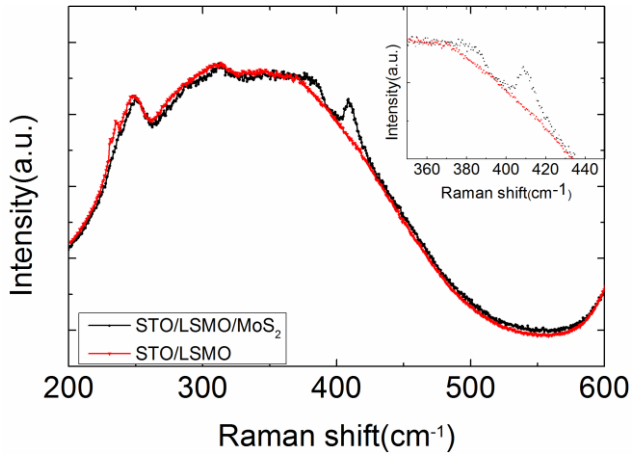

Fig.3 Raman spectra of STO/LSMO (20 nm) without (red curve) and with 2 nm of MoS_2 deposited on LSMO(black curve). Inset highlights the results between 370 cm^{-1} and 450 cm^{-1}.

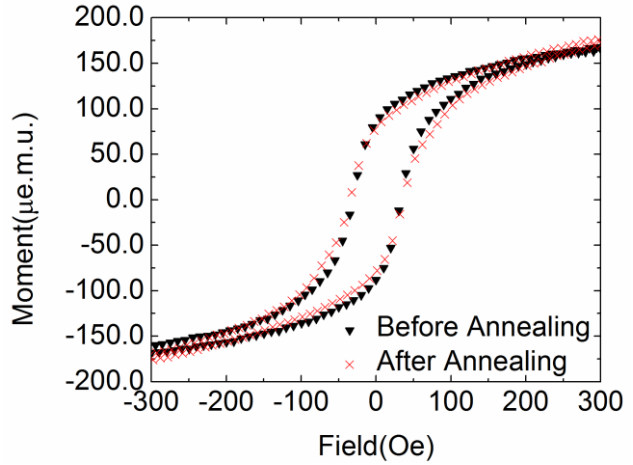

Fig.4 Hysteresis loops of STO/LSMO/MoS_2 sample before and after post annealing.

Conclusions

In conclusion, post-annealing of room temperature sputtered MoS_2 films yields samples with higher crystallinity, as compared with laser annealing and high temperature deposition. The MoS_2 production process does not affect the LSMO properties. When compared with other MoS_2 production process, sputtering shows a repeatable, mass production ready, and substrate independent route for the fabrication electronic and spintronic devices. Our results have demonstrated the feasibility of preparing such devices based on MoS_2 and perovskite oxides.

Acknowledgement

This work was supported by the Hong Kong Research Grant Council (PolyU 153015/14P) and the Hong Kong Polytechnic University (1-ZE14/1-ZVGH/G-YBJ1/G-YBPU).

References

[1] B. Radisavljevic, A. Radenovic, J. Brivio, V. Giacometti, and A. Kis, "Single-layer MoS_2 transistors," *Nat Nano,* vol. 6, no. 3, pp. 147-150, 2011.

[2] Q. H. Wang, K. Kalantar-Zadeh, A. Kis, J. N. Coleman, and M. S. Strano, "Electronics and optoelectronics of two-dimensional transition metal dichalcogenides," *Nat Nano,* vol. 7, no. 11, pp. 699-712, 2012.

[3] C. C. Liu, W. Feng, and Y. Yao, "Quantum spin Hall effect in silicene and two-dimensional germanium," *Phys Rev Lett,* vol. 107, no. 7, p. 076802, 2011.

[4] P. Vogt *et al.*, "Silicene: compelling experimental evidence for graphenelike two-dimensional silicon," *Phys Rev Lett,* vol. 108, no. 15, p. 155501, 2012.

[5] H. Liu *et al.*, "Phosphorene: an unexplored 2D semiconductor with a high hole mobility," *ACS Nano,* vol. 8, no. 4, pp. 4033-41, 2014.

[6] V. Tran, R. Soklaski, Y. F. Liang, and L. Yang, "Layer-controlled band gap and anisotropic excitons in few-layer black phosphorus," *Phys Rev B,* vol. 89, no. 23, p. 235319, 2014.

[7] Z. Yin *et al.*, "Single-layer MoS_2 phototransistors," *ACS Nano,* vol. 6, no. 1, pp. 74-80, 2012.

[8] B. Cho *et al.*, "Charge-transfer-based Gas Sensing Using Atomic-layer MoS_2," *Scientific Reports,* vol. 5, p. 8052, 2015.

[9] K. S. Novoselov *et al.*, "Electric field effect in atomically thin carbon films," *Science,* vol. 306, no. 5696, pp. 666-9, 2004.

[10] X. Cui *et al.*, "Multi-terminal transport measurements of MoS_2 using a van der Waals heterostructure device platform," *Nat Nano,* vol. 10, no. 6, pp. 534-540, 2015.

[11] J. Liu *et al.*, "Preparation of MoS_2-polyvinylpyrrolidone nanocomposites for flexible nonvolatile rewritable memory devices with reduced graphene oxide electrodes," *Small,* vol. 8, no. 22, pp. 3517-22, 2012.

[12] L. A. King, W. J. Zhao, M. Chhowalla, D. J. Riley, and G. Eda, "Photoelectrochemical properties of chemically exfoliated MoS_2," *Journal of Materials Chemistry A,* vol. 1, no. 31, pp. 8935-8941, 2013.

[13] Y. Zhan, Z. Liu, S. Najmaei, P. M. Ajayan, and J. Lou, "Large-area vapor-phase growth and characterization of MoS_2 atomic layers on a SiO_2 substrate," *Small,* vol. 8, no. 7, pp. 966-71, 2012.

[14] Y. H. Lee *et al.*, "Synthesis of large-area MoS_2 atomic layers with chemical vapor deposition," *Adv Mater,* vol. 24, no. 17, pp. 2320-5, 2012.

[15] S. Najmaei *et al.*, "Vapour phase growth and grain boundary structure of molybdenum disulphide atomic layers," *Nat Mater,* vol. 12, no. 8, pp. 754-9, 2013.

[16] Y. Y. Hui *et al.*, "Exceptional tunability of band energy in a compressively strained trilayer MoS_2 sheet," *ACS Nano,* vol. 7, no. 8, pp. 7126-31, 2013.

[17] W. Wang *et al.*, "Spin-Valve Effect in NiFe/MoS_2/NiFe Junctions," *Nano Lett,* vol. 15, no. 8, pp. 5261-7, 2015.

[18] M. E. McConney *et al.*, "Direct synthesis of ultra-thin large area transition metal dichalcogenides and their heterostructures on stretchable polymer surfaces," *Journal of Materials Research,* vol. 31, no. 07, pp. 967-974, 2016.

[19] H. Li *et al.*, "From Bulk to Monolayer MoS_2 : Evolution of Raman Scattering," *Adv Funct Mater,* vol. 22, no. 7, pp. 1385-1390, 2012.

[20] O. Takumi *et al.*, "Multi-layered MoS_2 film formed by high-temperature sputtering for enhancement-mode nMOSFETs," *Japanese Journal of Applied Physics,* vol. 54, no. 4S, p. 04DN08, 2015.

[21] M. I. Serna *et al.*, "Large-Area Deposition of MoS_2 by Pulsed Laser Deposition with In Situ Thickness Control," *ACS Nano,* vol. 10, no. 6, pp. 6054-61, 2016.

[22] M. S. Donley, P. T. Murray, S. A. Barber, and T. W. Haas, "Deposition and Properties of MoS_2 Thin-Films Grown by Pulsed Laser Evaporation," *Surface & Coatings Technology,* vol. 36, no. 1-2, pp. 329-340, 1988.

[23] H. F. Wong, K. Wang, C. W. Leung, and K. H. Wong, "Magnetoresistance of Manganite-Cobalt Ferrite Spacerless Junctions," *Ieee Transactions on Magnetics,* vol. 50, no. 7, pp. 1-4, 2014.